# RESULTS FROM A SOIL $CO_2$ FLUX AND SHALLOW TEMPERATURE SURVEY AT THE SAN JACINTO-TIZATE GEOTHERMAL POWER PROJECT, NICARAGUA

Mark C. Harvey[1], Phil J. White[1], Ken M. MacKenzie[1] and Brian G. Lovelock[1]

[1]Sinclair Knight Merz, Carlaw Park, 12-16 Nichols Lane, Parnell

mharvey@skm.co.nz

**Keywords:** *Soil, $CO_2$, flux, shallow, temperature, survey, geothermal, San Jacinto, Nicaragua.*

## ABSTRACT

A 609 point soil $CO_2$ gas flux and shallow temperature survey was undertaken to determine if mapped faults are associated with elevated $CO_2$ flux and/or shallow (≤1m) subsurface temperatures in an area of 20km$^2$ in and around the San Jacinto-Tizate geothermal power project, Nicaragua. The main objective of the survey was to assist with well targeting and help to refine the conceptual model of the San Jacinto-Tizate geothermal system. The survey confirmed the previously mapped NNE striking faults, and indicates that there is fairly widespread permeability on those faults, and also on the margin of a diorite intrusive which marks the eastern margin of the field. This survey also identified a previously unmapped NNE trending fault passing through the El Tizate area. In addition, a large area of anomalous $CO_2$ flux occurs on a major mapped fault to the west, and along with a magnetotelluric anomaly and distant thermal features provides additional evidence for the eastern extent of the western sector.

## 1. INTRODUCTION

### 1.1 Historical Background

A soil gas and temperature survey was previously undertaken at San Jacinto-El Tizate prior to the first round of drilling in 1993 (Ostapenko and Romero, 1995). Both soil $CO_2$ and temperature results from Ostapenko and Romero (1995) showed anomalies coincident with areas of surface thermal activity at San Jacinto and El Tizate.

### 1.2 Objectives

Surface thermal features (springs, steaming ground and small fumaroles) at San Jacinto and El Tizate occur at several low elevation locations near San Jacinto village and at El Tizate to the north. Soil gas flux and shallow temperature measurements provide additional tools for identification of faults and near surface heat flow, assuming that those faults allow greater fluid flow than elsewhere. As $CO_2$ is the major component of typical geothermal gases (including at San Jacinto), and is readily detectable, it is the most appropriate component to focus on.

The 2011 soil $CO_2$ gas flux and shallow temperature survey was undertaken to determine if areas of elevated $CO_2$ flux and/or elevated shallow (≤1m) subsurface temperature support the presence of mapped faults, and to identify other potential structural features that may be providing anomalous temperature and gas flux. Elevated $CO_2$ flux may indicate areas where degassing geothermal fluids are present in the subsurface and their upflow is focused on permeable structures. Shallow temperature anomalies are a direct indication of thermal activity (steam) that brings heat close to the surface.

The soil gas and shallow temperature survey was undertaken at the same time as a gravity and magnetic geophysics survey. The primary objectives of these surveys were to:

- Assist with targeting future production and injection wells. At the time of the survey, wells SJ11-1 and SJ12-3 were still to be completed. Both of these wells were planned as step out wells in the northern part of the resource, and the survey was intended to assist with targeting these wells.
- Provide additional information to assist with updating the conceptual model of the resource and the numerical reservoir model.

The 2011 soil $CO_2$ flux survey was different than the soil gas concentration survey of Ostapenko and Romero (1995). In 1995, in situ *concentrations* of $CO_2$ were measured. The 2011 soil $CO_2$ survey measured the $CO_2$ *flux* – that is, the mass of $CO_2$ (grams) flowing through a given cross-sectional area of soil (m$^2$) per unit of time (day). Ostapenko and Romero (1995) also measured temperatures at 1m, similar to this survey.

## 2. METHODS

### 2.1 Field Methods

The survey design had three primary components (Figure 1):

a) Grid pattern survey for identification of soil $CO_2$ flux and shallow temperature trends over a wide area.
b) Transects across identified and postulated faults and the margin of a diorite intrusive to confirm their existence, and permeability.
c) Extension of grid to additional areas if time allowed.

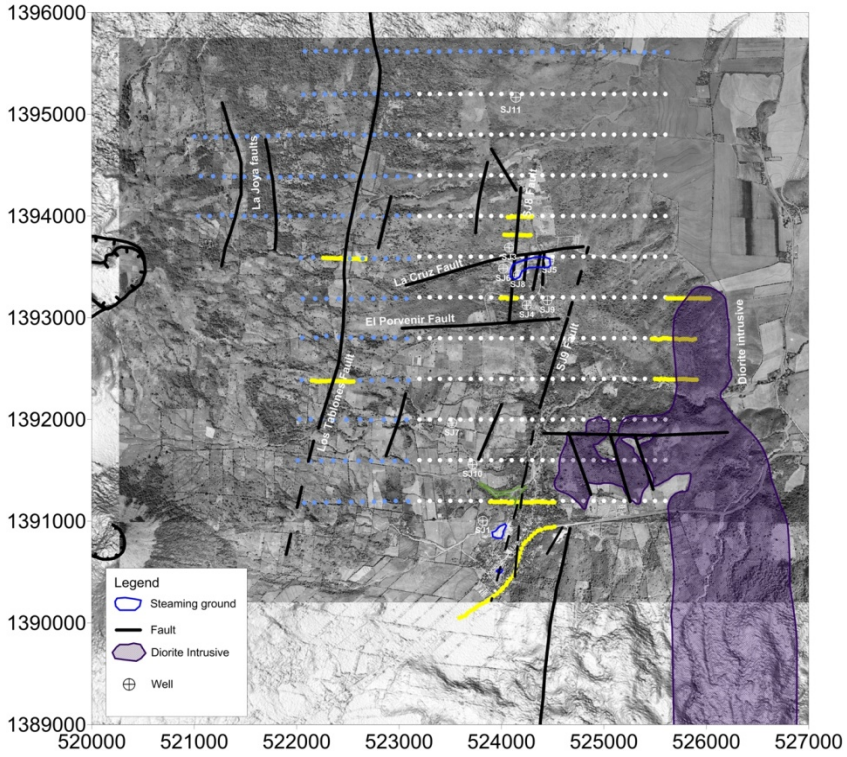


**Figure 1: Soil $CO_2$ flux and shallow temperature survey design. Note: white dots - grid pattern, blue dots - survey extension, yellow dots - high density transects.**

High priority target areas were identified for investigation and subjected to high density transect sampling (Figure 1):

a) NE trending structures mapped from aerial photographs, digital elevation models, surface geological mapping and drilling. These structures include Los Tablones fault, SJ8 fault, and the southern SJ9 fault in the vicinity of San Jacinto Village. Of these structures, the Los Tablones Fault shows clear offset of topography, indicating vertical movement, whereas most of the others are much more tentative. Elevated $CO_2$ flux across these features could identify permeability, and thus provide supporting evidence for the presence of faulting.

b) Major diorite intrusion identified from geological surface mapping and drilling. This intrusive is considered to form the eastern boundary of the hydrothermal system.

### 2.2 Field Measurement Techniques

609 soil $CO_2$ flux measurements were made using a calibrated West Systems portable soil gas flux meter (accumulation chamber method - Figure 2). The accumulation method calculates $CO_2$ flux by placing a 200 mm diameter accumulation chamber on the soil surface and pressing it into the soil to obtain a seal. Gases flowing into the chamber are pumped to an infrared gas analyser and the increase in $CO_2$ concentration inside the chamber over time is recorded by the instrument. The rate of concentration increase is proportional to flux.

Fluxes and temperatures were typically measured along high density transects at (~25 m point spacing), or as part of a 100 x 400m grid pattern (Figure 1).

For each site, soil temperature was measured with a handheld Type K thermocouple probe inserted to a maximum depth of 1m below ground level. The probe temperature was allowed to equilibrate for at least 30 seconds before each reading. Two probes were carried to allow cross checking of temperature measurements to verify measurement accuracy. The maximum depth to which the probe could be inserted depended on the density of the soil and rocks present at each individual location.

Thermal areas (fumaroles and springs) are present in close proximity to both SJ8 (El Tizate) and southern SJ9 faults (San Jacinto village). High density East-West transects were planned to avoid directly passing over these thermal areas as this technique is better suited to investigating areas with no obvious thermal activity.

### 2.3 Data Processing and Interpretation

Collected data was gridded for contouring using the Surfer© Kriging (soil $CO_2$ flux data) and Inverse Distance to a Power (shallow soil temperature data) algorithms. Grid sizes were 66 x 600 and 40 x 200 respectively. Temperatures at 0.5m provide a compromise between adequate depth (to avoid diurnal effects) and sufficient coverage (there are fewer deep measurements due to inability to probe to 1 m through rocky soils and outcrops).

In order to evaluate whether the soil $CO_2$ flux measurements were due to background biological soil conditions or geothermal sources, a cumulative probability plot was generated (Figure 3). Inflection points in cumulative probability plots can be used to distinguish the presence of multiple populations (Sinclair, 1974).

There is only one clear inflection point in Figure 3 (13 $g \cdot m^{-2} \cdot d^{-1}$) and this value probably represents the threshold between background biological $CO_2$ flux and geothermal flux at San Jacinto. This value is equal to the global mean background soil $CO_2$ flux for tropical environments (13 ± 6.8 $g \cdot m^{-2} \cdot d^{-1}$) (Bond-Lamberty and Thomson, 2010), which provides support to this argument.

Other inflection and break points in soil $CO_2$ flux data are ambiguous and further partitioning of statistical populations is not possible.

**Figure 2: Soil $CO_2$ flux measurement at San Jacinto, July 2011. $CO_2$ flux analyser is worn as a backpack, and accumulation chamber placed over soil.**

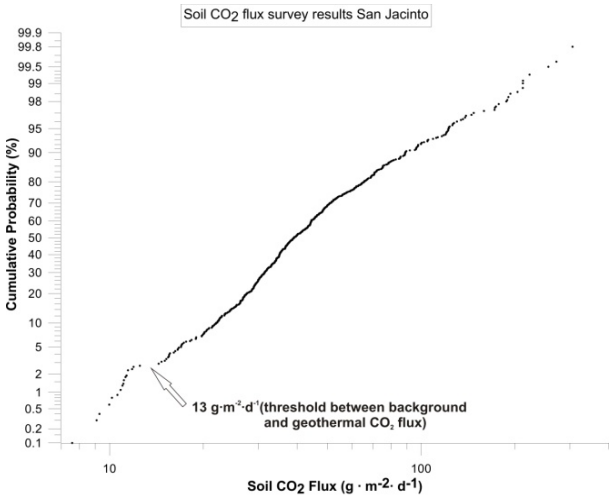


**Figure 3: Cumulative probability plot for soil CO2 flux.**

**RESULTS**

### 3.1 Soil $CO_2$ Flux

Soil $CO_2$ flux results are shown as point data in Figure 4. For clarity, only two levels (80 and 100 $g \cdot m^{-2} \cdot d^{-1}$) are used to classify the strength of the anomaly based on the measured gas flux at each measurement location.

**Table 1: San Jacinto soil gas flux anomaly classification**

| Description | $CO_2$ flux ($g. m^{-2} \cdot d^{-1}$) | Symbols |
|---|---|---|
| Weak anomaly and background | ≤ 80 | White dot |
| Moderate anomaly | 80 to 100 | Yellow dot |
| Strong anomaly | >100 | Orange dot |

Several key patterns are evident in Figure 4:

A. Clustering of $CO_2$ flux anomalies around San Jacinto village, and
B. around the El Tizate thermal area.
C. SJ9 and SJ10 faults both have several points along their length with $CO_2$ flux anomalies.
D. Los Tablones and La Joya faults are coincident with $CO_2$ flux anomalies.

Soil $CO_2$ flux results are shown as contoured data in Figure 5. Key anomalous areas are:

E. Clustering of strong $CO_2$ flux anomalies around San Jacinto village and El Tizate areas.
F. Distinct moderate to strong $CO_2$ flux anomalies found in several places along 4km of the Los Tablones fault. The anomaly is strongest in the central part, compared with the northern and southern ends of the fault, which may be outside the geothermal system.
G. A strong $CO_2$ flux anomaly close to the interpreted diorite intrusion and adjacent to Wellpad X. Reasonable correspondence exists between the western lobe of the interpreted diorite boundary and the 40$g \cdot m^{-2} \cdot d^{-1}$ flux contour.
H. The western interpreted La Joya fault is coincident with strong $CO_2$ flux anomalies where it was cut by two east-west transects approximately 1km apart.
I. A sequence of three closely spaced, moderate to strong anomalies forms a straight line that when extended, passes north through the El Tizate and SJ-10 well pad flux anomaly zones.
J. The postulated SJ9 and SJ10 faults have moderate to strong $CO_2$ flux anomalies at several points along their interpreted surface traces.

### 3.2 Shallow Soil Temperature

Soil temperature measurements were measured at 609 locations, where soil gas flux measurements were also collected. Contoured shallow soil temperature data at 0.5m are shown in Figure 6. Key anomalous areas are:

A. Strong shallow surface temperature anomalies around San Jacinto village and El Tizate thermal areas.

B. The western interpreted La Joya fault is coincident with a small temperature anomaly at the northern end.
C. Immediately west of the interpreted diorite intrusion close to where the diorite outcrops in El Apante gorge, near pad X.
D. East of SJ11, coincident with a soil $CO_2$ flux anomaly (Figure 5), and a smaller anomaly south of SJ11.

## 4. DISCUSSION

### 4.1 Soil $CO_2$ Flux

The presence of strong soil $CO_2$ flux anomalies nearby to San Jacinto village and Tizate thermal areas is consistent with results from a previous soil $CO_2$ survey at San Jacinto (Ostapenko and Romero, 1995), and with the obvious thermal activity in those areas. In both studies, strong anomalies are present in the area centred near the SJ-5 well pad at Tizate, and to the southeast of SJ-1 well pad at San Jacinto village. This latest survey significantly extends that previously undertaken in terms of coverage area and recognition of anomalies.

$CO_2$ flux is above background levels for most of the surveyed area. This is illustrated by the limited areas that fall below the 26 g· $m^{-2}$·$d^{-1}$ contour (see dark blue areas in Figure 5). This contour contains $CO_2$ fluxes within two standard deviations of the global mean background soil $CO_2$ flux for tropical environments. The wide area covered by above-background $CO_2$ flux is probably due to widespread diffusion of geothermal $CO_2$ in the survey area. Diffusive geothermal flux is only absent in isolated pockets, and in the north east of the survey area.

The SJ9 and Los Tablones faults were transected numerous times (10 and 8 times respectively) (Figure 1). Moderate to strong $CO_2$ flux anomalies were found at the intersection of both these faults in the majority of transects. This suggests that permeability extends over considerable distance (~4 and 3km respectively) for both faults (Figure 5).

The Los Tablones fault hosts a broad area of moderate to strong anomalous $CO_2$ flux midway along its length (Point F, Figure 5). It is possible that this area is the manifestation of the intersection of the Los Tablones fault with the EW striking El Porvenir and La Cruz faults. Alternatively, it could relate to the more northerly strike of this section of the Los Tablones fault here, and hence more extensional movement relative to the predominant NNE striking sections.

$CO_2$ flux anomalies in the mid-Los Tablones area, along with the La Joya faults to the west, are coincident with a significant doming of the base of the MT conductor (SKM, 2008) (Figure 5), and provide additional evidence for the eastern extent of the western sector. These anomalies indicate a substantial flow of $CO_2$ and by proxy, heat, just west of the El Tizate thermal area.

The eastern margin of the San Jacinto-Tizate geothermal system is marked by a diorite intrusion, at least in places. The reasonable correspondence between western lobe of the interpreted diorite boundary and the 40 g· $m^{-2}$·$d^{-1}$ $CO_2$ flux contour (Figure 5), along with the anomaly noted above, indicate permeability on that diorite contact.

A sequence of three closely spaced moderate to strong anomalies forms a straight line that passes through the SJ-10 well pad, and when extended, passes north through El Tizate and onto another $CO_2$ flux anomaly in the north, just east of well SJ-11 (Figure 5). The line also passes through four key shallow soil temperature anomalies (Figure 6), which suggest that this line comprises a previously unrecognised fault. This "SJ-10 fault" has the same NNE orientation as other major faults that cut across the San Jacinto geothermal system (e.g. Los Tablones, SJ8 and SJ9 faults).

$CO_2$ flux has been used as a proxy for steam and surface heat flow previously (i.e. Fridriksson et al. 2006):

$$Fstm,CO_2 = FCO_2 \times [H_2O] / [CO_2] \quad (1)$$

Where $Fstm,CO_2$ is the steam mass flow, in kg·$s^{-1}$, and $FCO_2$ is the mass flow of $CO_2$ in kg·$s^{-1}$, and $[H_2O] / [CO_2]$ = the ratio of the vapour phase supplying the thermal area. This calculation does not consider fluid/heat flow associated with the remaining brine fraction.

Equation (2) substitutes known reservoir fluid $CO_2$ content at El Tizate to derive reservoir fluid flow:

$$Fres,CO_2 = FCO_2 \times [RES] / [CO_2] \quad (2)$$

Where $Fres,CO_2$ is the reservoir fluid flow associated with measured $CO_2$ flux, $FCO_2$ is the mass flow of $CO_2$, and $[RES] / [CO_2]$ is the mass ratio of reservoir fluid to $CO_2$ measured from deep well discharges.

Note: $Fres,CO_2$ includes both steam and brine flows; steam separates from the brine and flows upward with $CO_2$, whereas the remaining brine fraction flows from the reservoir via another pathway. Flows along both pathways are relevant from the perspective of sustainable geothermal power generation.

Reservoir fluid flows and heat flows associated with the central Los Tablones fault and El Tizate $CO_2$ moderate to strong flux anomalies (areas ≥ 80 g· $m^{-2}$·$d^{-1}$, Figure 5) are estimated using the above equation and compared (Table 2).

**Table 2: Fluid and heat flow estimates based on $CO_2$ Flux**

| [1]Area | Area ($m^2$) | [2]$FCO_2$ (t/hr) | [3] $F_{RES}$ (t/hr) | [4]Heat $Flow_{(MWth)}$ |
|---|---|---|---|---|
| El Tizate | 205,000 | 0.98 | 980 | 326 |
| Los Tablones | 635,000 | 2.89 | 2890 | 965 |

[1]The 80g· $m^{-2}$·$d^{-1}$ contour is closely associated with the central Los Tablones fault and El Tizate thermal areas and is useful to constrain our estimate.
[2]$CO_2$ flow: assumes hydrothermal $CO_2$ flux = mean flux of Area, less background flux (13 g· $m^{-2}$·$d^{-1}$).
[3]Reservoir fluid flow associated with measured $CO_2$ flux: Assumes mass ratio [Reservoir Fluid] / $[CO_2]$ = 1000 based on sampling El Tizate deep wells. Includes steam and brine fractions.
[4]Assumes reservoir fluid enthalpy of 1200 kJ/kg based on sampling El Tizate deep wells. Note: Sub-surface heat flow may relate to boiling at depth occurring in vapour dominated zones, so does not require heat flow to the surface immediately above (i.e. coincident with the $CO_2$ flux anomaly).

It is important to note this survey was designed for wide area prospecting, and not to provide a quantitative estimate of heat flow in localized areas containing visible surface thermal activity (i.e. El Tizate, San Jacinto). Accordingly, no attempt was made to utilize shallow temperature measurements for heat flow estimation, and flows for El Tizate in Table 2 should probably be considered minimum values; The wide sample spacing means our results do not account for small zones of very high (convective) $CO_2$ fluxes likely to be present in these areas, and inclusion of the flux through discrete thermal features would probably add significantly to the total.

Equally, while the areal extent of the moderate to strong $CO_2$ flux anomaly at El Tizate is reasonably well constrained by the 80 $g \cdot m^{-2} \cdot d^{-1}$ contour, the anomaly at Los Tablones is unbounded to the west and may to be larger than estimated here (Figure 5).

Nevertheless, a comparison of flows (Table 2) suggests the moderate to strong Los Tablones $CO_2$ flux anomaly constitutes an area with three times the sub-surface fluid flow (and by proxy heat flow) of El Tizate (Table 2).

### 4.2 Shallow Soil Temperature

Strong shallow surface temperature anomalies around San Jacinto village and El Tizate areas (Figure 6) are consistent with those observed by Ostapenko and Romero (1995). In general shallow soil temperature corresponds to elevation, with cooler temperatures at higher elevation, as might be expected. However some anomalies that are clearly associated with geothermal heat flow are apparent.

A dashed line linking $CO_2$ flux anomalies (Figure 5) also links four key shallow soil temperature anomalies (Figure 6). This observation provides additional support for the existence of the newly defined "SJ-10 fault".

The western interpreted La Joya fault is coincident with a weak shallow soil temperature anomaly at the northern end (Point F, Figure 6). It is interesting that while strong shallow soil temperature anomalies are associated with the lower elevation $CO_2$ flux anomalies, they do not coincide with the $CO_2$ flux anomalies on Los Tablones or La Joya faults. The explanation is related to the depth of the geothermal reservoir in these locations. In the El Tizate area, the high reservoir pressure and shallow water table means that the deep reservoir is very close to the surface, and seasonal chloride springs confirm this. Furthermore, drilling shows that this area is close to the main geothermal upflow zone, where the reservoir is boiling, at least locally as it ascends, producing a higher steam flux. Hence $CO_2$ flux anomalies and temperature anomalies coincide. In the western area, the deep reservoir fluids are probably at greater depth because of the higher elevation terrain. Accordingly, little or no steam (and therefore heat) reaches the surface in this area because any steam condenses into cool subsurface aquifers; there are no surface thermal features associated with these faults. However $CO_2$, being relatively insoluble in water, passes through the shallow aquifers to reach the surface.

A temperature anomaly immediately west of the diorite intrusion may be associated with a $CO_2$ flux anomaly slightly to the north (Point G, Figure 6). These anomalies appear to result from an upflow of $CO_2$ and heat adjacent to the western margin of the diorite intrusive.

Smaller heat anomalies are present to the north of SJ8 fault and to the NNE of the SJ9 fault (Point H, Figure 6), and may indicate northward extension of these faults, beyond their mapped extents in the area near the SJ11 well pad. However, none of the points are coincident with $CO_2$ flux anomalies or mapped faults, suggesting these anomalies should be interpreted with caution.

## 5. CONCLUSIONS

The key outcome of the survey has been to demonstrate the effectiveness of the Soil $CO_2$ flux survey as a powerful and relatively inexpensive geothermal prospecting tool that allows:

- Confirmation of the location and permeability of suspected faults
- Identification of additional permeable structures.
- Identification of the more permeable parts of major structures.
- Identification of the existence of a geothermal system where thermal features are lacking.
- Confirmation of the lateral extent of a geothermal system.
- Estimation of total heat and fluid flow through permeable zones.

## ACKNOWLEDGEMENTS

We would like to acknowledge and thank Ram Power and Polaris Energy Nicaragua S.A. for allowing publication of the material presented in this report, and for the assistance of their site staff during the fieldwork. We would also like to thank Dr Clinton Rissmann at the University of Canterbury for his editorial input.

## REFERENCES

Bond-Lamberty, B.P. and A.M. Thomson. 2010. A Global Database of Soil Respiration Data, Version 1.0. Data set. Available on-line [http://daac.ornl.gov] from Oak Ridge National Laboratory Distributed Active Archive Center, Oak Ridge, Tennessee, U.S.A.

Fridriksson, T., Kristjansson, R., Armannsson, H., Margretardottir, E., Olafsdottir, S., Chiodini, G. (2006). $CO_2$ emissions and heat flow through soil, fumaroles, and steam-heated mud pools at the Reykjanes geothermal area, SW Iceland. Applied Geochemistry, 21(9): 1551-1569.

Ostapenko, S. V. and Romero, F. (1995) Levantamiento de gases del subsuelo y temperaturas superficiales en el campo geotermico San Jacinto-Tizate. Geotermia 11, 145-154.

Sinclair, A. J., Selection of threshold values in geochemical data using probability graphs, J. Geochem. Explor., 3, 129– 149, 1974.

Sinclair Knight Merz (2008) Geoscientific study and review of the San Jacinto Geothermal System. Client Report.

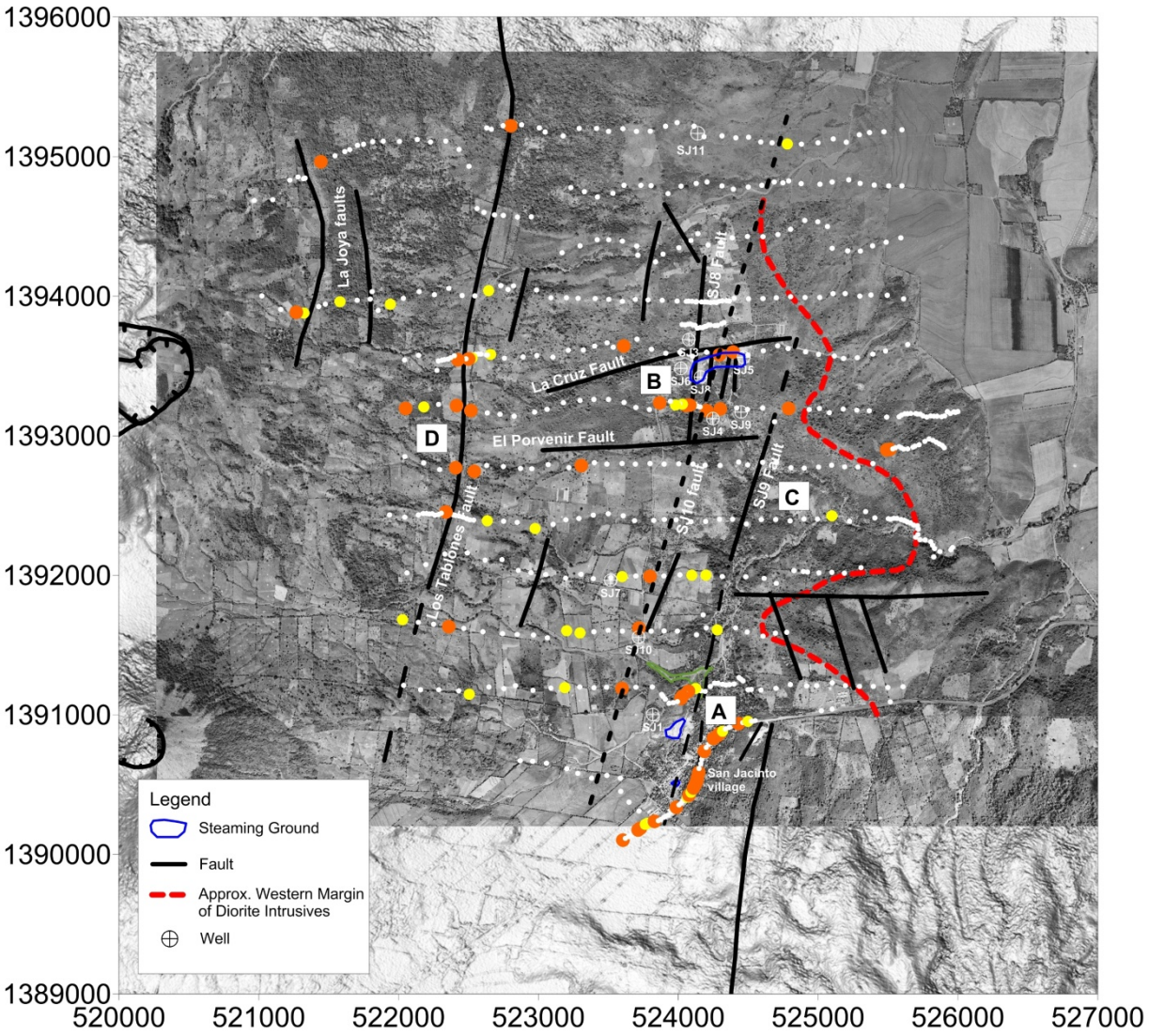


**Figure 4: Soil CO2 flux survey results. Note: small white dot (≤ 80g•m$^{-2}$•d$^{-1}$), yellow dot (80 - 100g•m$^{-2}$•d$^{-1}$), orange dot (>100g• m$^{-2}$•d$^{-1}$). See Section 3.1 for anomaly classification and explanation of areas A - D.**

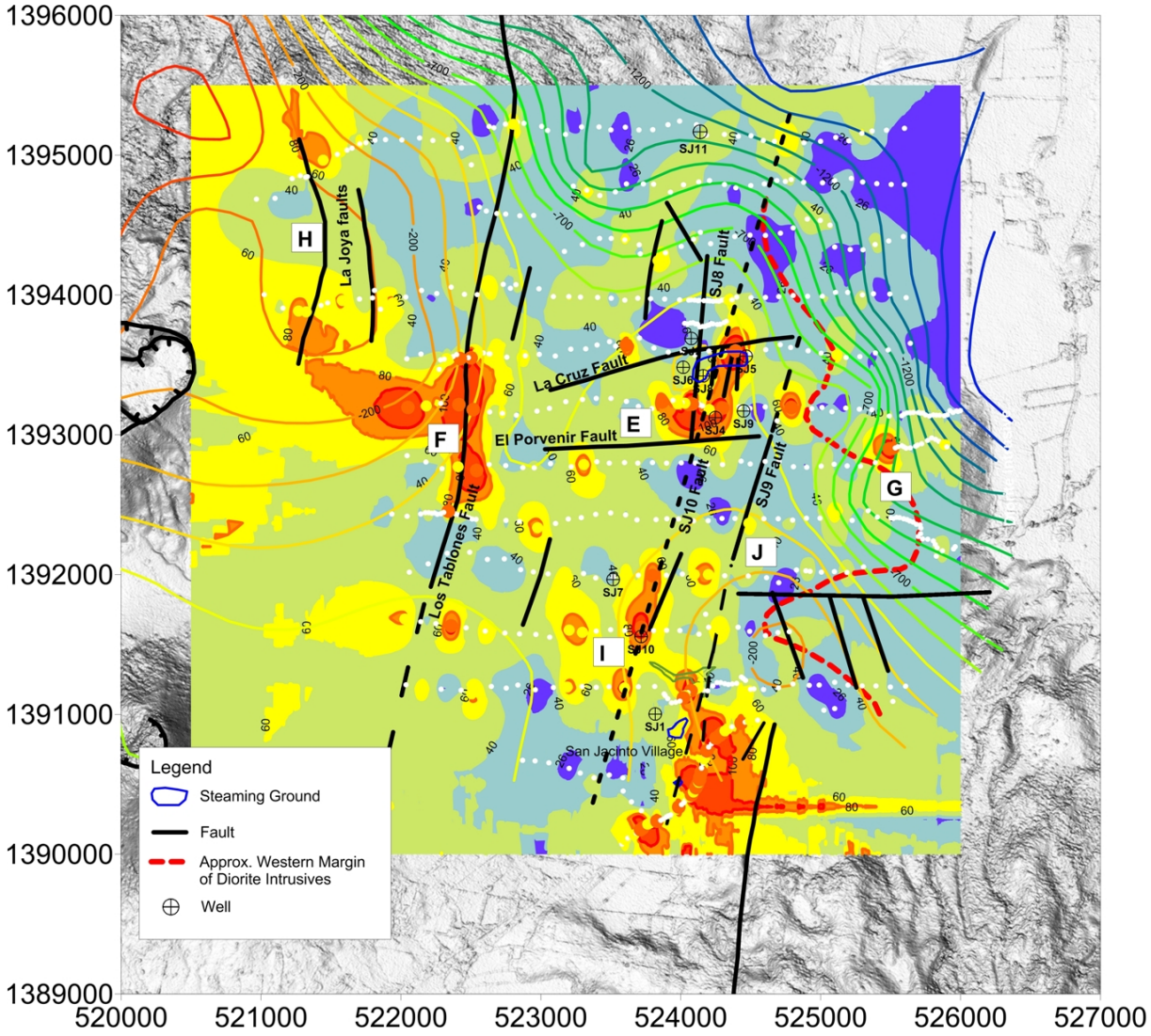


**Figure 5: Soil $CO_2$ flux (filled contours) with MT Base of conductor (unfilled contours) – 3D model (SKM, 2008). See Section 3.1 for explanation of locations E - J. White dots are soil $CO_2$ flux sampling locations.**

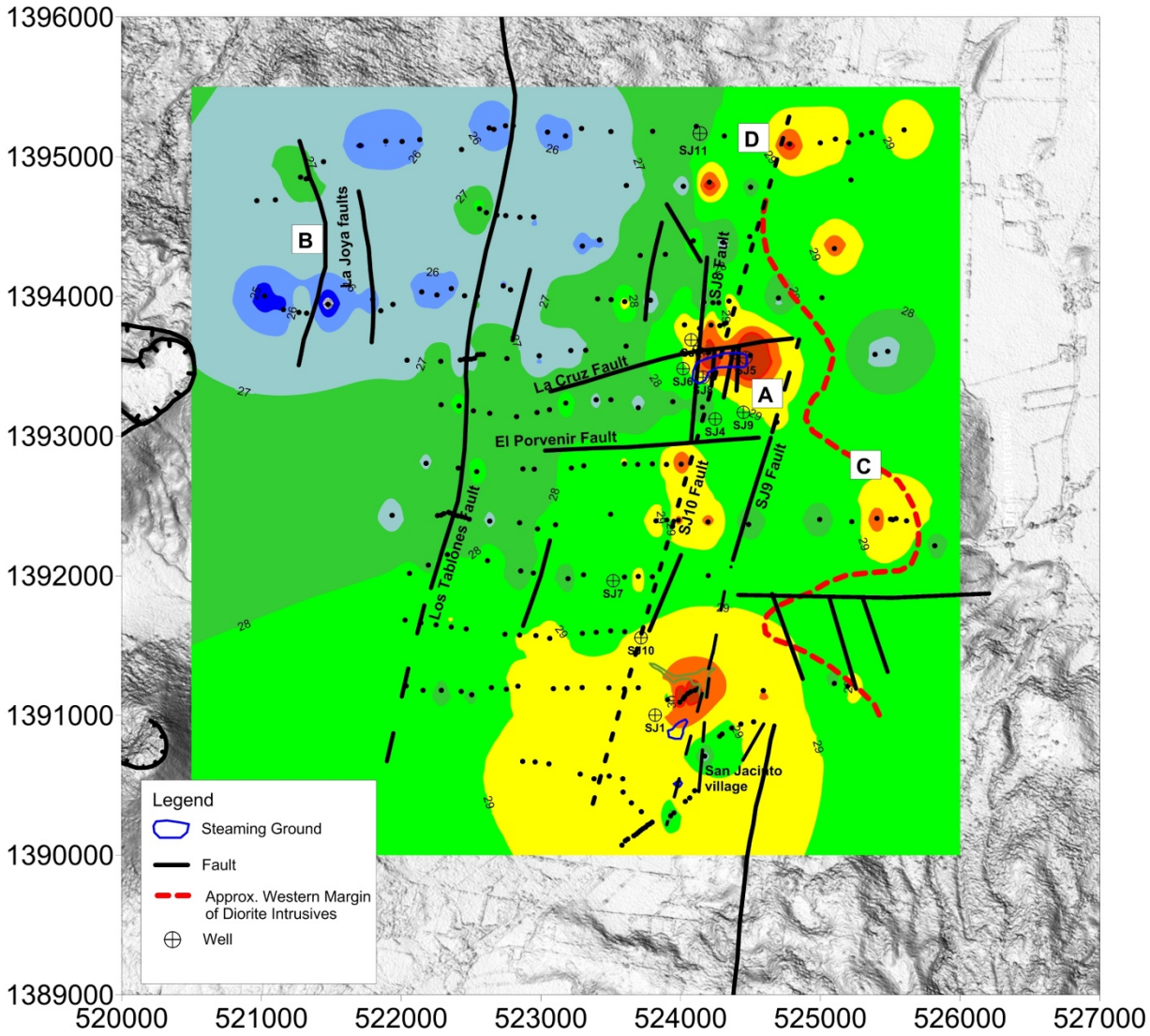


**Figure 6: Soil temperature contours at 0.5m (°C). See Section 3.2 for description of anomalies at A - D. Black points are measurement locations.**